ADS40 CALIBRATION BASED ON A TEST FIELD

TU Xinru, XU Miaozhong

State Key Laboratory for Information Engineering in Surveying, Mapping and Remote Sensing, Wuhan University, Wuhan, 430079, China-(tuxinru86@sina.com, miaox@lmars.whu.edu.cn)

Commission VI, WG VI/3

Keywords: ADS40; Photogrammetry; Calibration; Test Field; IMU Misalignment; Aerial Triangulation

ABSTRACT:

After a certain time, a calibration of ADS40 is essential, including determination of the coordinate assigned to each pixel in focal plate and IMU misalignment, so-named calibration file. There are two ways of calibration: laboratory calibration and test field calibration. The test field calibration leads to greater precision than the other one, because it is performed under realistic working conditions. In recent years, many papers focused on estimating the performance of the calibration file and the influence of self-calibration. Nevertheless, the goal of this paper was to generate a sufficient calibration file based on test field calibration.

In this paper, mathematic models involved with calibration were introduced, and a calibration workflow was developed, consisting of estimation, calibration and verification. All the experiment data was provided by Wuhan University, including calibration blocks acquired over Songshan Testsite in August 2009, while the certification of calibration file of ADS40 was provided in February 01,2007, and the coordinates of all the ground control points (GCPs) with an accuracy of 1cm. Based on the original calibration file, aerial triangulation was performed. Self-calibration improved accuracy of data processing obviously, which indicated the necessity of calibration. Then a new calibration file was generated, which was different from the original one. With two sets of data in different flight height, a comparison of performance between the original calibration file and the new one was made, which proved the latter one to be sufficient and reliable.

1. INTRODUCTION

Airborne photogrammetry is a fundamental and efficient technique for producing geospatial information. Calibrated sensors ensure the reliability and accuracy of airborne photogrammetry. There are two ways of calibration, including laboratory calibration and test field calibration. Normally, the latter one is considered to be a supplement to the former one.

ADS40 is airborne three-line scanner, integrated with GPS/IMU system, whose particular sensor geometry brings a particular data processing method and calibration, comparing to traditional frame sensor. ADS40 calibration is to determinate the coordinate of each pixel in focal plate and IMU misalignment, with the latter only can be solved by test field calibration (Schuster, 2000). The manufactory of ADS40 provides the calibration file, including so-named CAM file which defines the coordinate of each pixel in focal plate and IMU misalignment, which is generated by laboratory calibration and test field calibration. After a certain time, a calibration must be executed, because the status of ADS40 changes, which results in the error of calibration file.

Test field calibration is more flexible than laboratory calibration. People had done lots of research on test field calibration, for example, analyzing the systematic error and the way of compensation on the purpose of direct geo-referencing(Jacobsen, 2004), the performance of ADS40 with and without self-calibration(Casella, 2007), the calibration of IMU misalignment(Honkavaara, 2003). All that indicated the influence of calibration file to data accuracy.

A theoretical investigation of the resulting change of the focal length had been made (Meier, 1978). With the improvement of equipment stability, it is possible to generate a sufficient calibration file which is capable in a certain period based on test field calibration. The goal of this paper was to generate a sufficient calibration file based on test field. In this paper, mathematic models involved with calibration were introduced, and a calibration workflow was developed and executed.

2. MATHEMATIC MODEL

1.1 Transformation between Ground and Sensor

ADS40 is three line scanner with single lens. The integrated GPS/IMU system records the positions and attitudes with high frequency which can be translated to exterior orientation parameters.

Aerial triangulation can't be executed while exterior orientation parameters of each project centers are considered as unknowns. In this case, here comes "orientation fixes" at regular intervals along the flight path of ADS40 (Hinsken, 2002). The figure 1 shows the relation among ground point, project center, and orientation fixes. The project centers can be calculated by interpolation from the neighboring orientation fixes, which leads to the decrease of unknowns and the implement of aerial triangulation.

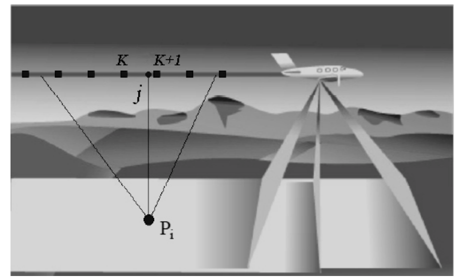

Figure 1. Correlation between Ground Point and Orientation Fixes

1.2 IMU Misalignment

IMU is inertial measurement unit, which can detect the rotating angular velocity and acceleration of vector. With integration and coordinate system transformation, the relative position and attitude of vector can be determined. It is physically impossible to align the axes of IMU and camera to be perfectly parallel. The angles between IMU system and camera system are defined as IMU misalignment (e_x, e_y, e_z).

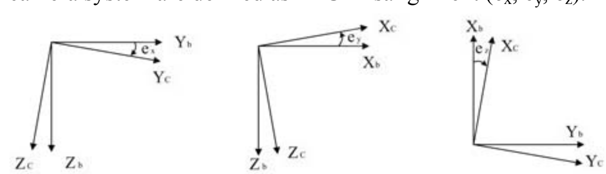

Figure 2. IMU Misalignment

The equation 1 describes the rotation from IMU to photogrammetric system.

$$R_b^C = R(e_x, e_y, e_z) = \begin{bmatrix} 1 & 0 & 0 \\ 0 & \cos e_x & -\sin e_x \\ 0 & \sin e_x & \cos e_x \end{bmatrix} \begin{bmatrix} \cos e_y & 0 & \sin e_y \\ 0 & 1 & 0 \\ -\sin e_y & 0 & \cos e_y \end{bmatrix} \begin{bmatrix} \cos e_z & -\sin e_z & 0 \\ \sin e_z & \cos e_z & 0 \\ 0 & 0 & 1 \end{bmatrix}$$
$$= \begin{bmatrix} \cos e_y \cos e_z & -\cos e_y \sin e_z & \sin e_y \\ \sin e_x \sin e_y \cos e_z + \cos e_x \sin e_z & -\sin e_x \sin e_y \sin e_z + \cos e_x \cos e_z & -\sin e_x \cos e_y \\ -\cos e_x \sin e_y \cos e_z + \sin e_x \sin e_z & \cos e_x \sin e_y \cos e_z + \sin e_x \cos e_z & \cos e_x \cos e_y \end{bmatrix} \quad (1)$$

To determinate the IMU misalignment, the bundle adjustment with a test field is necessary.

1.3 Brown Model

Various systematic effects in camera system is unavoidable, which needs to be compensated. Brown model (Brow, D.C.,

1976) focuses on the physical factors resulting in additional distortions and empirically performed well in various sensors calibration.

$$\begin{cases} dx = x_0 + a_1(r^2 - r_0^2)x + a_2(r^4 - r_0^4)x + a_3(r^6 - r_0^6)x \\ \quad + b_1 x + b_2 y \\ \quad + (c_1(x^2 - y^2) + c_2 x^2 y^2 + c_3(x^4 - y^4))x / c \\ \quad + d_1 xy + d_2 y^2 + d_3 x^2 y + d_4 xy^2 + d_5 x^2 y^2 \\ dy = y_0 + a_1(r^2 - r_0^2)y + a_2(r^4 - r_0^4)y + a_3(r^6 - r_0^6)y \\ \quad + (c_1(x^2 - y^2) + c_2 x^2 y^2 + c_3(x^4 - y^4))y / c \\ \quad + d_6 xy + d_7 y^2 + d_8 x^2 y + d_9 xy^2 + d_{10} x^2 y^2 \end{cases} \quad (2)$$

where c = Principal distance

x_0, y_0 = coordinates of principal point

a_1, a_2, a_3 = radial lens distortion parameters

b_1, b_2 = affinity and non-orthogonality parameters

c_1, c_2, c_3 = parameters for platen unflatness

$d_1 \cdots d_{10}$ = parameters for film deformations and non radial lens distortions

1.4 Aerial Triangulation with Additional Parameters

With all above, considering ground control points as weighted observations, the mathematic model of aerial triangulation is introduced:

$$\begin{cases} V_P = Ax_G + B_1 x + C_1 x_A - L_P, & P_P \\ V_C = E_C x_G - L_C, & P_C \\ V_{GPS} = B_2 x + C_2 x_{Dis} - L_{GPS}, & P_{GPS} \\ V_{IMU} = B_3 x + C_3 x_{Mis} - L_{IMU}, & P_{IMU} \\ V_A = E_A x_A - L_A, & P_A \end{cases} \quad (3)$$

where V_P, V_C, V_{GPS}, V_{IMU}, V_A = vectors of corrections to coordinates of image points, ground control points, GPS observation, IMU observation and additional parameters

x_G, x, x_{Dis}, x_{Mis} = vectors of corrections to coordinates of ground points, elements of exterior orientation, offsets between camera and GPS antenna, misalignment between IMU axes and camera axes

x_A = vectors of additional parameters

P_P, P_C, P_{GPS}, P_{IMU}, P_A = vectors of weight matrixes of corresponding observations

L_P, L_C, L_{GPS}, L_{IMU}, L_A = vectors of constant terms of corresponding error equations

E_C, E_A=unit matrix

The symbols left = coefficient matrixes of corresponding error equations.

3. MATERIALS AND METHODS

a) Calibration Blocks

Empirical investigation was made using calibration blocks provided by the state key laboratory of information engineering in surveying mapping and remote sensing (LIESMARS), Wuhan University.

The serial number of ADS40 being used was 30053, and the certification of calibration file consisted of IMU misalignment and so-named CAM file which defined the position of each pixel in focal plate was provided by Leica in February 01, 2007. All the blocks was acquired in August 2009, over Songshan Testsite, which is established by Wuhan University in Henan, China, with a network of targeted benchmarks with an accuracy of 1cm in both horizontal and vertical, which enable calibration at various scales:

(1) The large-scale test field (size 3km×3km) contains 99 ground control points, which are square targets of 0.4m×0.4m or 1m×1m, with an average interval of 300m.

(2) The media-scale test field (size 5km×5km) which includes the large scale test field contains 171 ground control points. The additional 72 ground control points are square targets of 1m×1m, with an average interval of 500m.

(3) The small-scale test field (size 8km×8km) which includes the large scale test field contains 214 ground control points. The additional 43 ground control points are square targets of 1m×1m, with an average interval of 800m.

b) Calibration Workflow

The workflow of ADS40 calibration based on test field includes estimation, calibration and verification.

(1) With the test data A, to contrast the result of aerial triangulation with additional parameters and without additional parameters, on purpose to estimate the necessity of calibration.

(2) With the test data B, to execute the calibration, and generate new calibration file.

(3) With the test data C, to execute aerial triangulation with original calibration files and new calibration files respectively, then with the comparison of their performances, to verify the sufficiency and reliability of the new calibration file.

Test field calibration is superior to laboratory calibration, but with the high correlation among inner orientation, exterior orientation and IMU misalignment and so on, which leads to some restrictions of data B. There are two example commended: a bi-directional line and a bi-directional cross line in the same height, with a number of ground control points available; a bi-directional line and a bi-directional across line which flown on a second flight level at 1.5 times the height of the first level. The latter becomes a standard calibration flight configuration (Tempelmann, 2003). Be differently, data C includes data sets with various flight heights and acquire times.

4. EXPERIMENT

a) Estimation

To estimate whether a calibration should be taken, a dataset was used, which consisted of 3 bi-directional strips with relative flight height of 600m, that one of them was cross strips, and 37 GCPs distributed in the aerial region (figure 3). As shown in table 1, without considering calibration file as weighted observations, aerial triangulation with different GCPs configuration was executed. It should be noticed that the posteriori sigma naught (sigma0) value was about 0.66 pixel, which was not appropriate. Also the RMS of check points was not in the range of predefined values. In contrast, considering calibration file as weighted observations, the data accuracy improved a lot.

No. of GCPs	Self-calibration	Sigma0	RMS of Check Points （m）		
			X	Y	Z
0	N	4.5	0.092	0.176	0.288
5	N	4.6	0.082	0.147	0.116
	Y	1.6	0.014	0.018	0.025
9	N	4.6	0.084	0.133	0.117
	Y	1.6	0.014	0.015	0.025

Table 1. Assessment of the 600 m flight

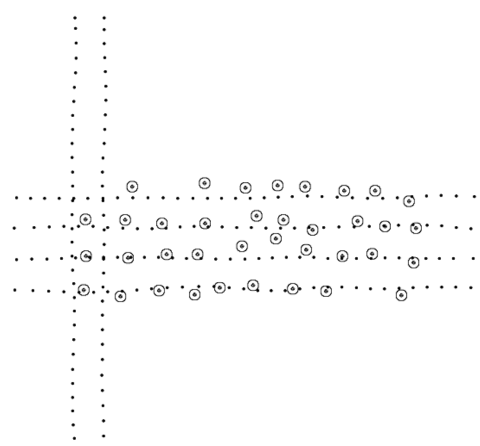

Figure 3. Structure of Data

b) Calibration

To generate a new calibration file, a calibration block was used, which consisted of four bi-directionally flown strips, forming crosses at two fight levels that one was 600m and another one was 1000m (figure 4).

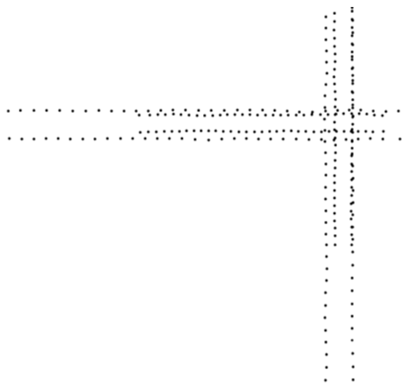

Figure 4. Structure of Data

With aerial triangulation, a new calibration file was generated, which contained the IMU misalignment and the coordinate of each pixel of five CCD arrays, including PANB14A, REDN00A, GRNN00A, BLUN00A and PANF28A. We numbered the original calibration file as V001, and the new one as V002.

As shown in table 2, there was a remarkable change of IMU misalignment in X and Y axis, while a relatively slightly change occurred in Z axis. The layout of five CCD arrays of V001 and V002 was shown in Figure 5, while the upper of it was the layout of entire CCD arrays, and the lower of it was the centre of CCD arrays with 8 times magnification. It was obviously that all the five CCD arrays didn't share the same shape. The CCD arrays of PANB14A and PANF28A were curves, while the other three were oblique lines. With calibration, the coordinates of all the pixels changed a lot. With the pixel size of 6.5μm, comparing to V001, all the five CCD arrays had slight shifts in Y axis, less than 1 pixel. Nevertheless, the shift of PANB14A in X axis was about 8 pixels, the shift of the three nadir CCD arrays was about 9 pixels, and the shift of PANF28A was about 11 pixels. There is no doubt that such a great change of calibration file would bring a significant effect to data accuracy.

calibration file	IMU Misalignment（rad）		
	O	P	K
V001	-0.00029493	0.011414004	-0.00209089
V002	-0.00012788	0.010650933	-0.00201749

Table 2. IMU misalignment (V001 VS V002)

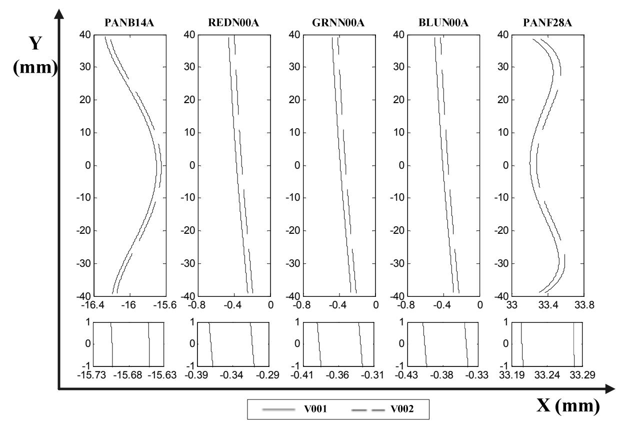

Figure 5. Location of ADS40's CCD Arrays in Focal Plate

c) **Verification**

In order to verify whether the calibration file V002 was sufficient and reliable, the following two dataset were selected:

(1) Dataset A: three bi-directional strips with the relative fight height of 600m, and overlap of 70%. There were 55 GCPs distributed in the aerial region.

(2) Dateset B: five parallel fight lines with the relative fight height of 1000m, and overlap of 60%. There were 94 GCPs distributed in the aerial region.

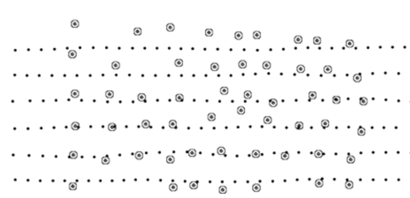

Figure 6. Structure of Dataset A

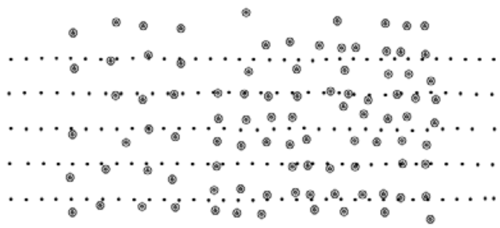

Figure 7. Structure of Dataset B

The workflow of verification was as follow: first, based on V001 and V002, the inner orientation of the flight data was carried out respectively. Then with different GCP configurations, aerial triangulation was done, which enabled a comparison in accuracy of check points.

Dateset A					
calibration file	No. of GCPs	Sigma0	RMS of Check Points（m）		
			X	Y	Z
V001	0	2.9	0.14	0.301	0.298
	5	3	0.121	0.215	0.329
	9	3.1	0.136	0.191	0.192
V002	0	1.7	0.019	0.026	0.132
	5	1.6	0.01	0.015	0.029
	9	1.6	0.01	0.015	0.022
Dataset B					
calibration file	No. of GCPs	Sigma0	RMS of Check Points（m）		
			X	Y	Z
V001	0	3.5	0.227	0.338	0.241
	5	3.5	0.194	0.29	0.35
	9	3.6	0.161	0.288	0.273
V002	0	1.6	0.033	0.029	0.088
	5	1.5	0.023	0.024	0.043
	9	1.5	0.018	0.019	0.039

Table 3. Assessment of the dataset A and dataset B

As shown in table 3, taken dataset A as test data, based on the original calibration file V001, with no GCPs used in aerial triangulation, the sigma0 value was more than half a pixel, and the RMS in planimetry ranged between 2.3 GSD and 5 GSD that the RMS in Y axis was almost twice than RMS in X axis. Meanwhile the RMS of Z axis was about 0.05% of relatively flight height. With 5 GCPs configuration, the sigma0 value had no improvement, in the other hand, the RMS in planimetry reduced, and the RMS in height increased. The use of 9 GCPs instead of 5 GCPs improved the data accuracy especially in height. The RMS in X axis was about 2.3 GSD, the RMS in Y axis was about 3.2 GSD, and the RMS in height was about 0.032% of the relative flight height. It should be noticed, that the RMS in Y axis always be larger than RMS in X axis, and with more GCPs introduced the disparity was weakened. In contrast, based on the modified calibration file V002, with no GCPs used in aerial triangulation, the RMS in X axis was about 0.3 GSD, and the RMS in Y axis was about 0.5 GSD. Meanwhile the RMS of Z axis was about 0.022% of relatively flight height. The sigma0 value was about a quarter of one pixel, which was almost a perfect value. With GCPs introduced, both 5 GCPs configuration and 9 GCPs configuration, the accuracy was perfect, that the RMS in planimetry was about 0.2 GSD and the RMS in height was about 0.004% of relative flight height. Obviously, there was a remarkable improvement of V002 compared to V001.

Just as dataset A, dateset B was processed. Compared to V001, based on V002, the sigma0 value and RMS in planimetry and in height had a significant improvement. In condition of data processing based on V001, the sigma0 value was more than half pixel with all three GCP configurations, and the best RMS in planimetry and in height were 1.6-2.9GSD and 0.027% of relative flight height. Nevertheless, with V002, the data accuracy performed excellent. While no GCP introduced, the sigma0 value was a quarter of one pixel, and the RMS in planimetry and in height were 0.3 GSD and 0.009% of relative flight height, respectively. The consideration of GCPs brought a slightly improvement of data accuracy in RMS.

The experiment results with dataset A and dataset B had something in common, that V002 leaded to an accurate and reliable data process, rather than V001. Because, with a long period, the status of sensor had been change a lot, and a calibration file which could reflect the practical condition of sensor ensured a high precision data process.

5. CONCLUSION

Integrated with GPS/IMU system, and 100% of forward overlap, ADS40 enables direct geo-referencing. In theory, aerial triangulation with few GCPs leads to high precision data. Calibration file has a great influence in data accuracy. In this paper, a calibration workflow based on test field was presented and executed. Based on test field calibration, there was a significant change of calibration file, which is sufficient to enable the data processing with high accuracy.

Tests are still needed in future, just as with different model of compensating image deformation to modify the calibration files, and to investigate the validity period of calibration files.

REFERENCES

Brown, D.C. 1976. The Bundle Adjustment – Progress and Prospects. International Archive of Photogrammetry, Com. III, Helsinki, Finland.

Casella, V., Franzini, M., Kocaman, S., Gruen, A., 2007. Triangulation and Self-calibration of the ADS40 Imagery: A Case Study over the Pavia Test Site. 8th Conference on "Optical 3D Measurement Techniques", Zurich, Switzerland, 9-12 July

Hinsken L., Miller S., Tempelmann U., Uebbing R., Walker A.S. 2002. Triangulation of the LH Systems' ADS40 using ORIMA GPS/IMU. International Archive of Photogrammetry, Remote Sensing and Spatial Information Sciences, Vol XXXIV Part 3A, Graz, Austria

Honkavaara, E., R. Ilves, J. Jaakkola, 2003. Practical results of GPS/IMU/Camera-system calibration. Proceedings of International Workshop: Theory, Technology and Realities of Inertial/GPS Sensor Orientation, Castelldefels, Spain, 22.-23.9.2003, unpaginated CD-ROM, 10 p.

Jacobsen, K., 2004. Direct integrated sensor orientation — pros and cons. International Archives of Photogrammetry, XX ISPRS Congress, Commission III, Istanbul, Turkey, pp. 829-835.

Meier, H.K., 1975. The effects of environmental conditions on distortion, calibrated focal length and focus of aerial survey camera. Presented at the Conference of Working Group on Image Geometry, Comm. I, ISP, Ottawa, 1975, 10 p.

Schuster, R., B. Braunecker, 2000. Calibration of the LH Systems ADS40 airborne digital sensor. International Archives of Photogrammetry and Remote Sensing, 33(1): 288-294.

Tempelmann, U., Hinsken, L., Recke, U., 2003. ADS40 Calibration & Verification Process. In: Proc. of Workshop: Theory, Technology and Realities of Inertial/GPS/Sensor Orientation, ISPRS WG I/5, Barcelona 2003, on CD-ROM, 6 p.

ACKNOWLEDGEMENTS

The research described in this paper was supported by LIESMARS Special Research Funding and the Open Research Fund Program (07-08) of LIESMARS, China.